Pharmacological Research - Natural Products 7 (2025) 100231

Contents lists available at ScienceDirect

Pharmacological Research - Natural Products

journal homepage: www.sciencedirect.com/journal/prenap

Quercetin from *Parinari curatellifolia* planch.ex benth differentially regulates Drosophila insulin-like peptides II and V in hyperglycaemic flies

Simeon Omale [a,i,*], John C. Aguiyi [a,i], Gwyn W. Gould [b], Aboi J.K. Madaki [c,i], Taiwo E. Alemika [d,i], Titilayo O. Johnson [e], Pam D. Luka [f], Chuwang J. Nyam [g], Nnaemeka E. Nnadi [h], Francis M. Agwom [d,i], Uchechukwu Ohaeri [i], Sunshine O. Ochala [i], Patricia T. Clement [i], John A. Parkinson [j,**]

[a] *Department of Pharmacology and Toxicology, University of Jos, Jos, Nigeria*
[b] *Strathclyde Institute of Pharmacy and Biomedical Sciences, University of Strathclyde, 295 Cathedral Street, Glasgow G1 1XL, United Kingdom*
[c] *Department of Family Medicine, College of Health Sciences, University of Jos, Jos, Nigeria*
[d] *Department of Pharmaceutical and Medicinal Chemistry, University of Jos, Jos, Nigeria*
[e] *Department of Biochemistry, College of Health Sciences, University of Jos, Jos, Nigeria*
[f] *National Veterinary Research Institute, Vom, Nigeria*
[g] *Department of Human Anatomy, College of Health Sciences, University of Jos, Jos, Nigeria*
[h] *Department of Microbiology, Plateau State University, Bokkos, Nigeria*
[i] *Africa Centre of Excellence in Phytomedicine Research and Development, University of Jos, Jos, Nigeria*
[j] *Department of Pure and Applied Chemistry, Thomas Graham Building, University of Strathclyde, 295 Cathedral Street, Glasgow G1 1XL, United Kingdom*

ARTICLE INFO

Keywords:
Parinari curatellifolia
Drosophila insulin-like peptide
Diabetes
Chromatography
Quercetin

ABSTRACT

Parinari curatellifolia Planch.ex Benth is utilised for the treatment of diabetes in Sub-Saharan Africa. However, the molecular mechanism of action and bioactive compounds are not fully known. While the current management of diabetes is efficacious, limitations still exist. The purpose of this study is to characterise the hypoglycaemic principle(s) of *Parinari curatellifolia* (PC) and its mechanism in Drosophila insulin-like peptide (DILP) gene expression. The solvent fractions from the leaf of PC were evaluated for hypoglycaemic effects and compared with metformin and glibenclamide (standard drugs) in type 2 diabetic *Drosophila melanogaster* (DM). We used column chromatography and gel-filtration techniques to obtain a pure sample. Bruker AVANCE-II+ 600 MHz and AVANCE NEO 800 MHz NMR spectrometers were used to characterise the pure compound. The samples were run in duplicate for DILP2, DILP3, and DILP5 gene expression on BioRAD CFX96 RealTime PCR. Ethyl acetate fraction was as effective as metformin and glibenclamide in reducing the hyperglycaemic state in diabetic flies and a 50 % decrease ($p < 0.05$) in the glucose compared to the diabetic untreated (DU) control flies. The bioactive compounds of PC exhibit a 40 % and 70 % increase ($p < 0.05$) in DILP2 and DILP5 gene expression, respectively. The pure sample was characterized, and designated as Quercetin, a flavonol with molecular formula $C_{15}H_{10}O_7$. Quercetin from the leaf of *P. curatellifola* exhibits hypoglycaemic effects and increased DILP2 and DILP5 gene expression in diabetic DM like metformin and glibenclamide antidiabetics. This insight could guide drug development in the management of type 2 diabetes.

1. Introduction

The global spending to treat diabetes and its complications was US $760 billion in 2019 and is projected to increase to US $825 billion by 2030 [1]. Diabetes has a high contribution to deaths caused by other diseases [2]. Management approaches have improved diabetes care,

Abbreviations: DILCP, Drosophila Insulin-Like Peptides; PC, *Parinari curatellifolia*; CC, Column Chromatography; TLC, Thin Layer Chromatography; DM, Diabetes Mellitus; LDL, Low-Density Lipoprotein; ACEPRD, Africa Centre of Excellence in Phytomedicine Research and Development; DU, Diabetic Untreated; NMR, Nuclear Magnetic Resonance Spectroscopy.

* Corresponding author at: Department of Pharmacology and Toxicology, University of Jos, Jos, Nigeria.
** Corresponding author.
E-mail addresses: omales@unijos.edu.ng (S. Omale), john.parkinson@strath.ac.uk (J.A. Parkinson).

https://doi.org/10.1016/j.prenap.2025.100231
Received 24 September 2024; Received in revised form 14 April 2025; Accepted 15 April 2025
Available online 17 April 2025

however, several limitations still persist. Researchers are examining the role of natural products in managing diabetes [3]. Several medicinal plants have been investigated for their hypoglycaemic properties [4].

Parinari curatellifolia Planch. ex Benth (PC), a plant species widely used in traditional medicine, has been found to exhibit hypoglycaemic properties in various studies [5]. Another study reported the multiple therapeutic uses in traditional medicine [6]. The effects of the ethanolic extract of the stem bark of *P. curatellifolia* have been investigated against cobra venom-induced blood pressure in cats and rabbit jejunum [7]. Flavonoids from the seed of *P. curatellifolia* have been reported to exhibit anti-hyperlipidemic and anti-atherogenic effects on triton-induced dyslipidemia in rats [8]. The seeds of *P. curatellifolia* reduce plasma glucose levels in alloxan-induced diabetic rats [9]. The antioxidant properties of the seed extract of *P. curatellifolia* have been proposed as a possible mechanism of anti-diabetic action [10]. The hepatoprotective effects of flavonoids from *P. curatellifolia* against acetaminophen-induced necrosis in rats have been investigated [11], with extracts of fresh leaves having been reported for pain management, anti-inflammatory, and anti-neoplastic properties in Jurkat-T-cells [12]. Ogbonnia *et al.*, [13] reported decreased plasma glucose levels and low-density lipoprotein (LDL) in alloxan-induced diabetes in rats. Whether the extracts of *P. curatellifolia* exert effects on the insulin peptides or insulin receptors as a possible mechanism of action in type 2 diabetes remains substantially unknown. We have shown that the extract from *P. curatellifolia* exerts apparent hypoglycaemic effects in diet-induced diabetes in the *Drosophila melanogaster* [14]. Still, the possible mechanism and phytoconstituent(s) remain to be investigated.

The Drosophila model of type 2 diabetes has substantially contributed to cardiovascular and endocrine research [15,16]. *D. melanogaster* provides a convenient and suitable model to study drug mechanisms to evaluate anti-diabetes candidate drugs [17], and the Drosophila insulin-like peptides (DILP) and Drosophila insulin receptors (DInR) are known to perform similar functions to the mammalian homologs [18]. Here, we quantify glucose levels in the fly homogenates treated with the solvent fractions of *P. curatellifolia* to answer our research question. We also evaluate the active fraction against DILP2, DILP3, and DILP5 to understand if the hypoglycaemic effects of the active fraction modulate the Drosophila insulin peptides.

The chromatographic and spectroscopic techniques used in this work have been widely used previously to purify and characterise phytoconstituents from medicinal plants [19].

2. Materials and methods

2.1. Plant material

The leaf of *Parinari curatellifolia* (Local names: Rura, Enenchila; English name: Mobola-plum, cork tree, hissing tree) was obtained in the wild from Oiji Ochekwu, Apa Local Government Area of Benue State, Nigeria, in November 2020. The location is at a latitude between 78° and 8° north of the equator and about 8° on longitude east of Greenwich meridian. The location is within the geographical region of the Niger-Benue Trough, which is characterized by rich alluvial soil that supports the growth of aerial trees. The plant was authenticated in the Department of Agric Extension Services, Federal College of Forestry Jos, Nigeria. The herbarium specimen was prepared and deposited in the Department of Pharmacognosy, Faculty of Pharmaceutical Sciences, University of Jos, Nigeria, with the voucher specimen number UJ/PCG/HSP/11C26. The plant name was checked with the official website http://www.worldfloraonline.org and verified to correspond with the latest version (http://www.worldfloraonline.org. Accessed on: 06 Aug 2024). The leaves were air-dried at room temperature and pulverized to a fine powder. One thousand grams (1000 g) of the powder was extracted in 70 % ethanol with cold maceration for 72 h.

2.2. Fly stock and culture

The Harwich strain of *D. melanogaster* was obtained from the Drosophila laboratory of the Africa Centre of Excellence in Phytomedicine Research and Development (ACEPRD), University of Jos, Nigeria. The flies were maintained on standard Drosophila cornmeal medium consisting of brewer's yeast 1 % (w/v), methylparaben (0.08 %), agar (2 % w/v), and cornmeal 30 %. A constant temperature (24 ± 1°C) with 60 % relative humidity and a 12-h light cycle was maintained throughout the experimental period. Young flies of 2–3 days old were collected under CO_2 anaesthesia from the stock vials and divided into seven groups of 50 flies (both genders). The flies were flipped into new vials containing fresh food every three days to ensure food quality consistency.

2.3. Induction of type 2 diabetes

Very high carbohydrate or caloric diets have been used to study type 2 diabetes in the *D. melanogaster*. We used 2.5 g sucrose per /10 g diet regimen to induce diabetes in this experiment as described by Tennessen *et al.*, [20]. The experimental design involves exposing groups 2–7 of the naïve flies to a high sugar supplanted diet for ten days, while other ingredients (yeast 1 %, methylparaben 0.08 %, agar 2 %, and corn meal 30 %) were kept constant, and group one was maintained on the standard fly food without any supplementation. This diet leads to type 2 diabetes as exemplified by hyperglycaemia, insulin resistance, cardiac dysfunction, obesity, decreased locomotive performance, and decreased survival as reported in our previous experiment [14].

2.4. Activity-directed isolation and purification

We used an activity-guided protocol to first check the effects of the leaf extract of PC on type 2 diabetic flies by exposing the flies (groups 4–7) to graded concentrations of the crude extract (10 mg, 50 mg, 100 mg, 200 mg) per 10 g diet for hypoglycaemic effects. Groups 1 and 2 served as normal control and diabetic untreated (DU) respectively, while group 3 was treated with metformin 8 mg/10 g diet and as a standard control. Findings from this experiment led to the solvent partitioning of the crude extracts in a separating funnel for the ethyl acetate, n-butanol, n-hexane, and chloroform using a schematic approach (Fig. 1). The solvent fractions (water soluble and water insoluble) were evaluated in the diabetic flies for their hypoglycaemic effects. The solvent fractions with insufficient yield could not be evaluated for their anti-diabetic effects. Striking hypoglycaemic effects were observed with the ethyl

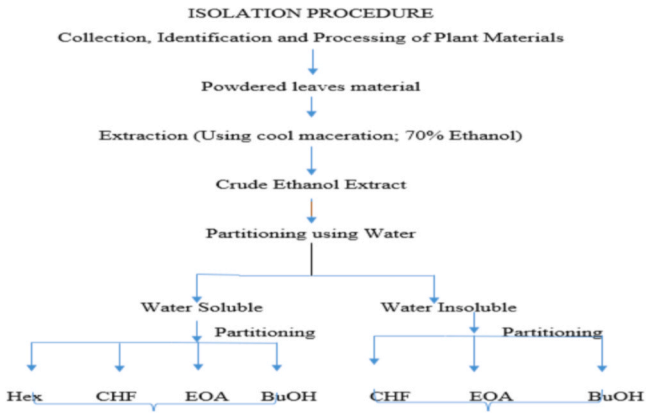

Fig. 1. Schematic Design for *Parinari curatellifolia* Leaf Extraction and Partitioning. The scheme of events for partitioning and fractionation using solvents of different polarities was followed to obtain distinct fractions, leading to the isolation and purification of a pure compound. Compounds of different polarity are partitioned according to their solvent's affinity variation.

acetate (water soluble and insoluble) solvent fraction. From these results, it was proposed that the anti-diabetic constituents of PC possibly reside more within the ethyl acetate solvent fraction. Theoretically, the biological activity of the active fractions will increase as the biologically active compounds become the larger part of the fraction [21]. We, therefore, proceeded with bio-assay guided fractionation using column chromatography incorporated with silica gel as the stationary phase and absolute methanol as the mobile phase to obtain the refined anti-diabetic active fraction of PC. Several fractions were obtained and labeled A- G. Further fractionation of the biologically active fractions yielded sub-fractions A1, A2, A3, A4……A25, …….G1,G2,G3,G4…… 34. The fractions were subjected to Thin Layer Chromatography (TLC) using silica gel 60 F254 20 by 20 cm aluminium plates. The subfractions with similar TLC profiles were pooled together and further subjected to antidiabetic assay in type 2 diabetic flies. Activity-directed fractionation was then used to purify the most active portion in a gel separation technique with Sephadex LH-20 as the stationary phase. Eluents were collected at the rate of one drop every 30 s in a 10 mL beaker and 2 mL per beaker. Fractions with similar profiles were subsequently pooled together and run through gel filtration for further purification. We ultimately obtained two pure compounds from the ethyl acetate portion of PC and coded them as PC1 and PC2. The pure isolated compounds yielded 34 mg and 3.5 mg respectively for PC1 and PC2, and were sent to the Department of Pure and Applied Chemistry, Thomas Graham Building, University of Strathclyde, 295 Cathedral Street, Glasgow, G1 1XL for full structural characterization and elucidation using NMR spectroscopy. Due to the inherently insensitive nature of NMR, there was insufficient PC2 for the spectroscopic analysis to progress very far for this compound However, it was possible to proceed with PC1.

2.5. Determination of the glycaemic status

The glycaemic status of the fly homogenate was determined using the Randox Gluc-Pap assay kit; Randox Laboratory Crumlin County Antrim, United Kingdom, based on the glucose oxidase assay method according to the manufacturer's protocol as previously described [14]. The samples were diluted in 1 μL:6 μL sample to PBS (0.01 M, pH 7.4) ratio to form the sample solution. The sample solutions of the individual experiments and the glucosidase reagent were mixed in a ratio of 1:9 μL and incubated at 25 °C for 25 min. The orange colour resultant products were read at 540 nm using the Jenway spectrophotometer version 7315, Cole-Parmer Ltd., United Kingdom.

2.6. NMR spectroscopy studies

The sample was subsequently prepared for NMR spectroscopy investigations by solubilizing the isolated product (4.3 mg dry weight) in 550 μL CD_3OD, following which the greenish-yellow solution was admitted to a high-precision (Wilmad 535-PP) 5 mm diameter NMR tube ready for analysis.

Solution-phase NMR spectroscopy data acquisition was done using the following protocols and parameters using NMR spectrometers operating at two different magnetic field strengths. NMR data were initially acquired at a magnetic field strength of 14.1 T using a Bruker AVANCE-II$^+$ 600 NMR spectrometer equipped with a Bruker Ultrashield standard bore magnet and operating at a proton resonance frequency of 600.13 MHz. A 5 mm broadband observe probe head equipped with an actively shielded gradient coil (Bruker probe head BBO-z-ATM) was used for subsequent NMR data acquisitions and was equilibrated at a probe head temperature of 298 K for all data accumulations.

1D ^{1}H NMR data were acquired with a single pulse-acquire pulse sequence (Bruker pulse program zg) over a frequency width of 7211.54 Hz (12.0166 ppm) centred at a resonance offset frequency of 3000.65 Hz (5 ppm) using a 12 μs 90-degree radio-frequency (r.f.) pulse calibrated at a pulse power of 23.76 W (-13.76 dB). Data were acquired using a relaxation delay of 2.0 s into 32768 data points for an acquisition time of 2.272 s with 32 transients and 2 dummy transients.

Again, NMR data were acquired with power-gated decoupling with a 30-degree pulse (Bruker pulse program zgpg30) over a frequency width of 37878.789 Hz (250.99 ppm) centred at a resonance offset frequency of 15090.28 Hz (100 ppm) and calibrated for a 90-degree ^{13}C r.f. pulse of duration 8.66 μs at a pulse power of 70 W (-18.45 dB). Data were acquired using a relaxation delay of 0.7 s into 32768 data points for an acquisition time of 0.433 s with 3072 transients and no dummy transients. Proton decoupling was applied centred at a proton offset of 4 ppm throughout the relaxation delay (0.698 W, 1.56 dB) and acquisition period (0.351 W, 4.54 dB) using a waltz16 composite pulse decoupling scheme.

Multiplicity-edited, Pure Shift 2D [^{1}H, ^{13}C] HSQC NMR data were acquired using a traditional sampling scheme (Bruker pulse program hsqcedetgpsisp2.3_bbhd) according to an echo/anti-echo acquisition protocol. Data were acquired into 2048 complex data points in ω_2 over a ^{1}H frequency width of 7211.539 Hz (12.0166 ppm, acquisition time = 142 ms) centred at 3000.65 Hz (5 ppm) and over a frequency width in ω_1 over a ^{13}C frequency width of 25655.658 Hz (170 ppm) centred at 12826.74 Hz (85 ppm). Data were acquired with 4 transients for each of 186 t_1 increments, which was sufficient to achieve good separation of all resonances in ω_1 upon Fourier transformation of the data. Acquisition was optimized for a $^1J_{HC}$ coupling of 145 Hz, and Pure Shift in ω_2 was achieved using an L0 value of 7 for a partial proton coupling evolution/refocusing period, d62 = 20.28 ms. Pulsed-field gradients used to select for coherence and spoiling were set according to the pulse program instructions. ^{13}C decoupling was achieved during the data acquisition period using the MPF9 composite pulse decoupling scheme.

2D [^{1}H, ^{13}C] HMBC NMR data were acquired using optimizations for $^nJ_{HC}$ = 12.0 Hz, 7.0 Hz, and 3.0 Hz with a non-uniform sampling scheme, NUS (Bruker pulse program hmbcgplpndqf). Data were acquired in 1024 complex data points in ω_2 over a ^{1}H frequency width of 1798.561 Hz (3.0 ppm, acquisition time = 285 ms) centred at 4200.91 Hz (7 ppm) and over a frequency width in ω_1 over a ^{13}C frequency width of 15092.394 Hz (100 ppm) centred at 21126.39 Hz (140 ppm). Data were acquired with NUS using 25 % of 1024 t_1 increments with 8 transients each and reconstructed to 1024 increments using the provided iterative soft thresholding reconstruction algorithm.

2D [^{1}H, ^{1}H] NOESY NMR data were acquired with a classical phase-sensitive approach (Bruker pulse program noesygpph). Data were acquired into 1024 complex data points in ω_2 and 256 data points in ω_1 over a ^{1}H frequency width of 1798.561 Hz (3 ppm, acquisition time in ω_2 = 285 ms) centred at 4100.91 Hz (7 ppm). Data were acquired with 8 transients for each of the 256 t_1 increments. A mixing time τ_m = 1.0 s was applied to allow NOE build-up to occur.

Further NMR data were subsequently acquired at a magnetic field strength of 18.8 T using a Bruker AVANCE NEO 800 NMR spectrometer equipped with an actively pumped 2.2 K standard bore magnet and operating at a ^{1}H resonance frequency of 799.43 MHz. A triple resonance, multinuclear observe, helium cryoprobe (Bruker probe head TXO-z) equipped with a single axis, actively shielded z-field gradient coil was used for all subsequent data accumulation at an equilibrated probe head temperature of 300 K.

1D ^{1}H NMR data were accumulated using Bruker pulse program zg30 with 32 transients and 2 dummy transients over a frequency width of 9615.385 Hz (12.03 ppm) into 65536 data points centred at a proton resonance frequency of 3996.15 Hz (5 ppm) for an acquisition time of 3.41 s with a relaxation delay of 3.0 s between transients.

NMR data were acquired with power-gated decoupling using Bruker pulse program zgpg30 with 16 transients and 4 dummy transients over a frequency width of 52631.578 Hz (261.8 ppm) centred at a carbon-13 frequency of 22112.41 Hz (110 ppm). Proton decoupling was applied centred at a proton frequency offset of 5596.01 Hz (7 ppm) using a waltz16 composite pulse decoupling program.

2D [^{13}C, ^{13}C] INADEQUATE NMR data were acquired using a traditional acquisition scheme and a States-TPPI acquisition mode using

Bruker pulse program inadphsp. Data were acquired over a carbon-13 ω_2 frequency width of 20 kHz (99.48 ppm, acquisition time = 205 ms) and ω_1 frequency width of 40.21 kHz (200 ppm, acquisition time = 2.3 ms) into 8192 and 184 data points, respectively. Each increment was acquired with 256 transients using a recycle delay of 5.0 s. The data accumulation was optimized for $^1J_{CC} = 50$ Hz. The total data accumulation period was 68 h.

All NMR data from either spectrometer were processed offline within TopSpin version 4.0.5 running on a 64-bit Windows 10 HP EliteOne 800 G3 desktop computer equipped with an Intel Core i5–7500 CPU operating at 3.4 GHz. NMR spectra were referenced to the residual solvent signal of methanol-d_4 at δ ^{1}H = 3.31 ppm ($CH\underline{D}_2OD$) and δ ^{13}C = 49.0 ppm ($\underline{C}D_3OD$).

2.7. DILP gene expression studies

Diabetes-relative gene expression studies of *P. curatellifolia* extract were investigated as follows. Diabetic *D. melanogaster* (both genders) were divided into six groups of 50 flies each. Group one was maintained as diabetic untreated (DU), group two was exposed to metformin (8 mg/ 10 g diet), group three was exposed to glibenclamide (0.05 mg/10 g diet), while groups four, five, and six were exposed to PCE 10 mg, 50 mg, and 100 mg/ 10 g diet respectively for seven days. Twenty fly heads per group were decapitated and homogenised in phosphate buffer saline (pH 7.0). The total mRNA of the DILP from insulin-producing cells was isolated from the head of the flies using Trizol (Invitrogen). The integrity and concentration of RNA were checked using Quibit4. The cDNA was generated from the total mRNA using the iScript cDNA synthesis kit (Bio-Rad). The iScript reactions were normalized to 1 ng and samples were run in duplicate for differential gene expression of target genes (DILP2, DILP3 and DILP5) with GAPDH as endogenous control on a Bio-Rad CFX96 RealTime PCR system. Expression differences and association of the genes and the control were analysed.

2.8. Statistical analysis

GraphPad statistical software version 9.3.1 was used for all the statistical analyses, setting the confidence level at 95 %. Ordinary One-way ANOVA and group comparison were deployed to test the mean between both negative and positive control groups and between treatments. Multiple analysis was used to compare among treatment groups. A p-value less than 0.05 was considered statistically significant and is indicated by an asterisk with automatic pairwise comparison.

3. Results

3.1. Activity-guided antidiabetic studies

The percentage yield from the crude maceration was 47 % (470 g) dry weight. Diet-induced hyperglycaemia and insulin resistance have been used to study type 2 diabetes in the *Drosophila melanogaster* with great success. Our experiments manifest classical signs of type 2 diabetes in the flies signified by hyperglycaemia, obesity, decreased survival rate, and locomotive deficit consistent with our previous reports. To evaluate the anti-hyperglycaemic effects of the crude extract of the leaf of PC, we carried out several pilot studies to determine the appropriate concentrations (data not shown). Based on the results of the safety pilot study, we determined that 10 mg, 50 mg, 100 mg, and 200 mg per 10 g diet was appropriate for the crude extract experiment. The anti-diabetic effects of PC leaf crude extract showed a significant decrease in the circulating ($p < 0.05$) glucose levels in all the diabetic-PC treated groups compared with the diabetic untreated (DU). Strikingly, there was no significant difference between the PC treated groups and their metformin treated group (Fig. 2).

The anti-diabetic assay for the ethyl acetate, n-butanol, and n-hexane was determined using the glucosidase method. We employ 1 mg, 10 mg,

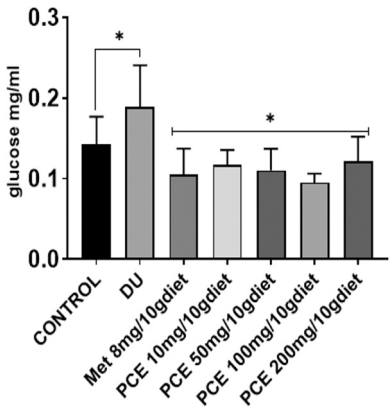

Fig. 2. Graded dose of the crude extract of the leaf *Parinari curatellifolia* (PC) reduces hyperglycaemia in the diabetic *Drosophila melanogaster* (DM). The experimental design involves exposing groups 2–7 of the naïve flies to a high sugar supplemented (sucrose 2.5 g) diet for ten days to induce type 2 diabetes, while other ingredients were kept constant. Group one was maintained on the standard fly food without any supplementation. To check for the antidiabetic effects of the *Parinari curatellifolia* extract, flies' groups 4–7 were exposed to graded concentrations of the crude extract (10 mg, 50 mg, 100 mg, 200 mg) per 10 g diet. Groups 1 and 2 served as normal control and diabetic untreated (DU) respectively, while group 3 was treated with metformin 8 mg/10 g diet and as standard control. All the PC-treated groups showed a significant decrease ($^*p < 0.05$) in hyglycaemic status of the diabetic flies compared to the DU group, while there was no statistical difference between the non-diabetic and metformin-treated groups. Among the PC-treated treatments, there is no statistical difference between groups.

50 mg, and 100 mg /10 g diet regimens due to safety concerns with doses above 100 mg/10 g diet. The toxicity symptoms could be attributed to an increased concentration of phytochemicals due to refined portion post fractionation. The ethyl acetate water-soluble (EtAsol) and water-insoluble (EtAins) fractions exhibited significant ($p < 0.05$) hypoglycaemic effects in the circulating glucose level of the diabetic treated compared with the diabetic untreated (DU) flies. However, there were no statistical differences between the EtAsol and EtAins-treated groups and the metformin-treated group. Interestingly, we also observed no statistical difference between the EtAsol and EtAins-treated and the non-diabetic flies (Fig. 3A & 3B). Decreased circulating glucose levels in the fly homogenates have been widely used to study the antidiabetic potential of substances in *D. melanogaster* [22]. However, the butanol water-soluble (Butsol) fraction showed abnormally increased ($p < 0.05$) circulating glucose levels in the diabetic flies. We speculate this to be due to the alcohol content of n-butanol that could have added to the hyperglycaemic state of the flies (data not shown). We also evaluated the hexane water-soluble (Hexsol) fraction in the diabetic flies and found no statistical difference ($p > 0.05$) between the DU and Hexsol-treated groups (data not shown). The yield from n-butanol and n-hexane water insoluble was not sufficient for biological activity experiments. Solvent partitioning, due to variations in polarity, accounts for product yield. The chloroform fraction was toxic to the flies even at low concentrations. Thus, we could not continue with the experiment.

3.2. NMR spectroscopy

Five ^{1}H NMR resonances were observed, each integrating to one proton equivalent (Fig. 4A): δ ^{1}H = 7.732 ppm (**A**: d, J_{HH} = 2.15 Hz, *meta* $^4J_{HH}$), δ ^{1}H = 7.630 ppm (**B**: dd, J_{HH} = 2.15 Hz, *meta* $^4J_{HH}$, J_{HH} = 8.47 Hz, *ortho* $^3J_{HH}$), δ ^{1}H = 6.884 ppm (**C**: d, J_{HH} = 8.44 Hz, *ortho* $^3J_{HH}$), δ ^{1}H = 6.386 ppm (**D**: d, J_{HH} = 2.09 Hz, *meta* $^4J_{HH}$), δ ^{1}H = 6.182 ppm (**E**: d, J_{HH} = 2.09 Hz, *meta* $^4J_{HH}$) (Fig. 4A). By contrast, the 1D ^{13}C-{^{1}H} NMR spectrum (Fig. 4B) showed 15 unique resonances, suggesting the likelihood of **1** belonging to the sesquiterpenoid class of

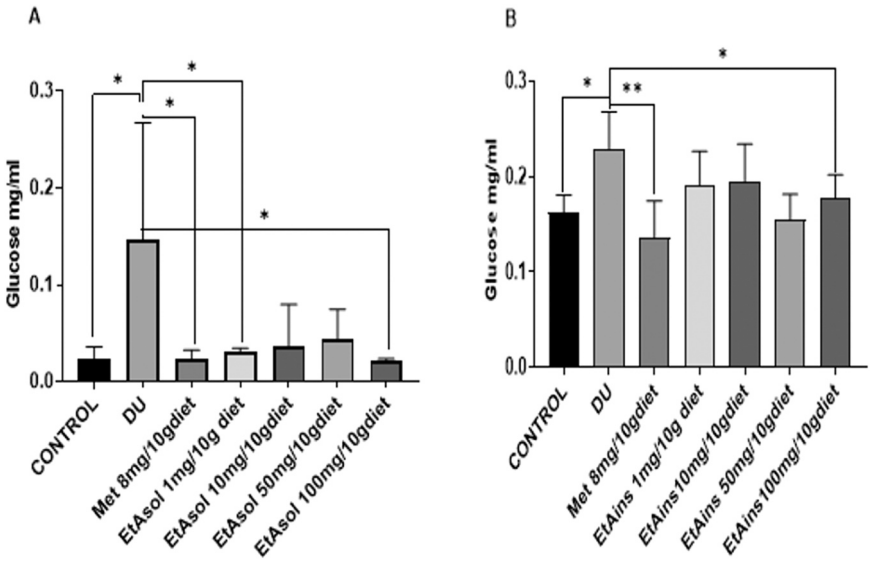

Fig. 3. Solvent fractions of the leaf of PC modulate hyperglycaemia in type 2 diabetic flies. **(A)** Sustained hyperglycaemia was observed in DU. This was ameliorated by MET, a standard oral hypoglycaemic drug. While there was no significant difference ($p > 0.05$) between the groups that received antidiabetic drugs and the EtAsol, there was a significant decrease ($p < 0.05$) in the glucose levels of the treated compared with DU. Similarly, there was no significant difference between the non-diabetic group and the treated and in between treatment groups. **(B)** The standard treatment showed decreased glucose levels compared to the DU, while only the 50 mg EtAins group showed a significant decrease ($p < 0.05$) in the glucose level compared to the DU.

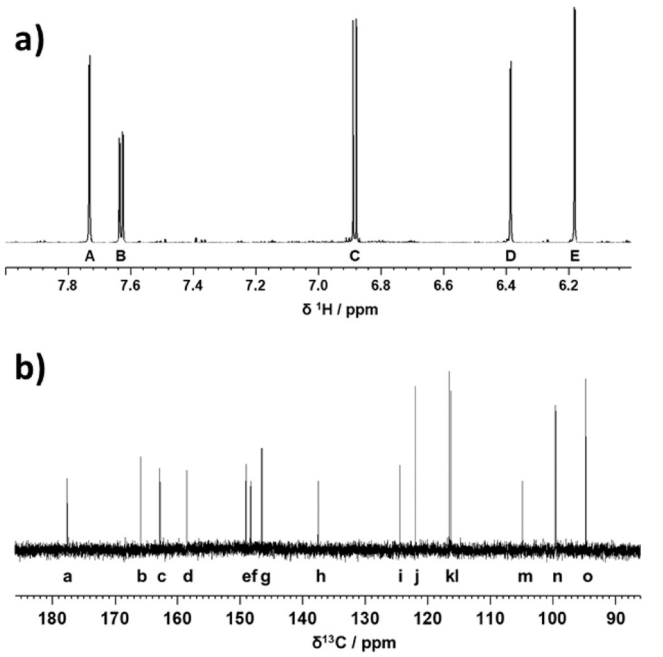

Fig. 4. 1D NMR spectra of 1. a) 600 MHz 1D ^{1}H NMR spectrum. Signals are labelled A – E and chemical shifts and coupling constants are defined according to the text. b) 1D ^{13}C-{^{1}H} NMR spectrum of 1 acquired at 18.4 T (200 MHz for ^{13}C observation). Signals are labelled **a-o** for assignment purposes.

molecules with a C_{15} carbon framework. Carbon-13 NMR resonances appeared at chemical shifts δ ^{13}C / ppm = 177.33 (**a**), 165.57 (**b**), 162.50 (**c**), 158.23 (**d**), 148.77 (**e**), 148.01 (**f**), 146.22 (**g**), 137.22 (**h**), 124.15 (**i**), 121.68 (**j**), 116.23 (**k**), 116.00 (**l**), 104.52 (**m**), 99.24 (**n**) and 94.41 (**o**). Of these, resonances **j**, **k**, **l**, **n** and **o** were of greater intensity compared with the remaining ten signals (Fig. 4B).

Inspection by 2D [^{1}H, ^{13}C] HSQC NMR spectroscopy confirmed these resonances to be associated with carbon centres bound directly to protons through single bonds and were thus correlated through $^{1}J_{HC}$ coupling as shown (Fig. 5A). To assist with understanding the carbon framework of **1**, 2D [^{13}C, ^{13}C] INADEQUATE NMR data were acquired and used to directly map the carbon-carbon skeleton of the molecule through $^{1}J_{CC}$ couplings and is summarized in the connectivity information following according to the labelled ^{13}C-{^{1}H} NMR signals in Fig. 4**b**: (**a**, **h**), (**a**, **m**), (**b**, **n**), (**b**, **o**), (**c**, **m**), (**c**, **n**), (**d**, **m**), (**d**, **o**), (**e**, **g**), (**e**, **k**), (**f**, **i**), (**g**, **l**), (**i**, **j**), (**i**, **l**) and (**j**, **k**). All these data were combined to deduce the structure and identity of **1** as detailed in Section 4.2 NMR spectroscopy discussion.

Comparison between calculated and experimental NMR results are reported in Table 1. Experimental results for a sample of Quercetin solubilized in CD_3OD and analysed by carbon-13 NMR spectroscopy at different magnetic field strengths [25] is also included.

3.3. *DILP gene expression studies*

The Drosophila insulin-like peptide 2 (DILP2) and Drosophila insulin-like peptide 5 (DILP5) are two principal hormones produced by the insulin-producing cells of the adult Drosophila brain to respond to sugar and protein metabolism. To understand the mechanism of action of PC on type 2 diabetes, we investigate the effects of PC solvent fraction on the expression of DILP2, DILP3, and DILP5 during hyperglycaemia in the *D. melanogaster*. Our results showed that the PC 50 mg/10 g diet significantly expressed DILP2 above the control. The standard drugs, metformin and glibenclamide, showed significant changes in the peptide (Fig. 8A). We speculate that PC might be acting *via* a more interesting mechanism that could be of benefit clinically. Effects of PC on DILP3 were not significantly different ($p > 0.05$) from the DU, but glibenclamide, an insulin sensitizer, increased the expression of the peptide (Fig. 8B), while there was a striking increase ($p < 0.05$) in the expression of the DILP5 in the flies exposed to PC 10 mg and 50 mg per 10 g diet respectively (Fig. 8C). DILP2 and DILP5 are involved in the homeostasis of carbohydrates and protein, including fats. This observation justifies the hypoglycaemic effects of PC in type 2 diabetes. DILP2 and DILP5 are highly conserved between Drosophila and man [18]. The similarity between human and insulin signalling pathways presents a strong benefit for the use of Drosophila to investigate potential anti-diabetic drugs.

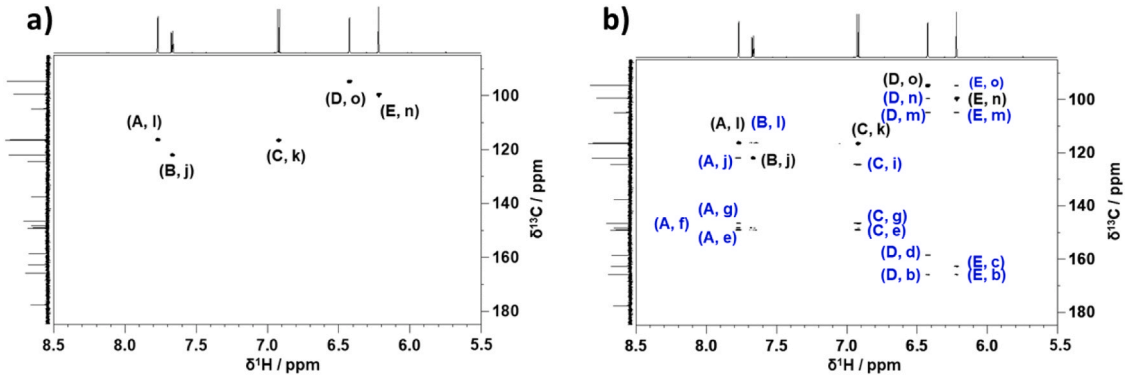

Fig. 5. 2D [^{1}H, ^{13}C] correlation maps for 1. a) 600 MHz 2D [^{1}H, ^{13}C] Pure Shift HSQC NMR spectrum. The five correlations are labelled according to the resonance lettering scheme used to annotate the 1D ^{1}H and ^{13}C-{^{1}H} NMR spectra shown in Fig. 4. **b)** Overlay of 600 MHz 2D [^{1}H, ^{13}C] Pure Shift HSQC and 2D [^{1}H, ^{13}C] HMBC NMR data for 1 in which HMBC data were optimized for $^{n}J_{HC} = 7$ Hz (n > 1). Black labels correspond to HSQC correlations as shown at **a)**. Blue labels correspond to HMBC correlations.

Table 1
Comparison of experimental and calculated carbon-13 chemical shifts for 1.

Assignment	Atom No.‡	δ^{13}C / ppm (Exptl)	δ^{13}C / ppm (Reported)[25]	Δδ^{13}C / ppm†	δ^{13}C / ppm (Calcd)*	δ^{13}C / ppm (Calcd)**	δ^{13}C / ppm (Calcd)***
A	4	177.33	176.5	0.83	176.6	176.1	177.4
B	7	165.57	166.0	−0.43	164.5	166.4	165.1
C	8a	162.50	161.0	1.50	156.8	158.8	160.8
D	5	158.23	156.7	1.53	163.1	161.8	157.7
E	4’	148.77	148.1	0.67	146.3	146.5	148.5
F	2	148.01	147.5	0.06	145.0	146.9	147.2
G	3’	146.22	145.7	0.52	145.8	145.9	145.4
H	3	137.22	136.5	0.72	137.08	136.5	136.3
I	1’	124.15	123.0	1.15	122.1	122.8	122.5
J	6’	121.68	121.0	0.68	127.7	121.8	120.7
K	5’	116.23	116.5	−0.27	115.8	117.2	115.8
L	2’	116.00	116.0	0.00	115.3	115.3	115.6
M	4a	104.52	104.0	0.52	105.1	104.5	103.2
N	8	99.24	99.5	−0.26	95.8	94.0	99.5
O	6	94.41	94.5	−0.09	101.1	98.3	94.4

†Chemical shift difference between experimental data (this work) and reported experimental data [25]; *Calculation using the web-based tools at www.nmrdb.org. **Calculation using ChemDraw. ***Calculation using Mnova. ‡Atom numbering according to the definitions provided [26].

4. Discussion

4.1. Antidiabetic properties of Parinari curatellifolia

Diabetes Mellitus has become one of the world’s most challenging health issues of the twenty-first century. The drug development process from herbal or alternative medicine, among others, involves bioassay-guided fractionation, isolation, and characterisation to separate complex mixtures of plant extracts [29]. From our bioassay-guided experiment, the Ethyl acetate fraction showed significant ($p < 0.05$) antidiabetic effects and was used to purify the antidiabetic compound, which was then sent for elucidation and characterization. The purification of compounds from natural products has long been used to identify novel therapeutic molecules [29]. *Parinari curatellifolia* has been deployed in alternative medicine in the management of diseases such as diabetes, cancer, diarrhoea, pneumonia, and fractures, mostly in Sub-Saharan Africa [6,8,10,11]. Extracts and phytochemicals from *P. curatellifolia* have been shown to improve type 2 diabetes [6,10,13]. We used the *Drosophila melanogaster* laboratory model to characterise possible anti-diabetic compounds from the leaf of PC. This could serve as a reliable and safe source of antidiabetic molecules, particularly for low-income countries. Orthodox antidiabetics alongside lifestyle changes have been used to manage diabetes with appreciable success, but they are not entirely effective with a complete cure. This has necessitated the continuous search for a more potent antidiabetic molecule globally. Our findings suggest that PC contains substances with profound antidiabetic properties that can be harnessed through structure-activity relationships (SAR) for antidiabetic drug development.

Recent advances in alternative medicine showed great potential for the treatment of various diseases, particularly using simple but versatile models such as *Drosophila melanogaster*. *D. melanogaster* has been used to understand the mechanism of action of various drugs used to treat human diseases [22]. Here, we used *D. melanogaster* to compare the effects of compounds of PC with metformin in type 2 diabetic flies and found a close resemblance in their activity.

4.2. NMR spectroscopy

Initial indications, based on the 1D ^{1}H NMR spectrum, showed the likelihood of the unknown compound, PC**1**, being aromatic in character with no aliphatic component. Through *J*-coupling alone, it was immediately apparent that resonances **A**, **B,** and **C** formed a spin system arranged according to an *ortho/para* trisubstituted aromatic ring and resonances **D** and **E** formed a *meta*-related pattern associated with a second aromatic ring system. The data in Fig. 5A allow the identification of CH partners connected through single bonds. When combined with through space correlation information, evident from 2D [^{1}H, ^{1}H] NOESY NMR data (**A** and **B** both show correlations to **D**, data not shown) an understanding of the relationship between the two fragments, ***A*** and ***B***, of **1**, with identification of the CH pairs, began to materialise (Fig. 6A).

The NOE correlations were particularly valuable, suggesting proximity between protons **A** and **D** and between protons **B** and **D**. No equivalent proximity to proton **E** was in evidence. This supported

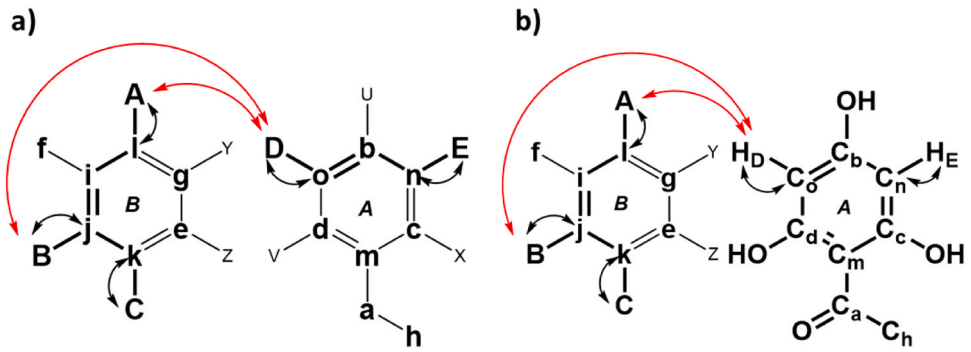

Fig. 6. Data to structure assignment. a) Assignment of ^{13}C NMR signals applied to a provisional atom arrangement according to labelled NMR signals and arranged according to $^{1}J_{CC}$ couplings as revealed through 2D [^{13}C, ^{13}C] INADEQUATE NMR data. **b)** Extension of fragment *A* based on chemical shift arguments as defined in the text.

evidence for a carbon-carbon bond existing between carbons bearing labels X and V in Fig. 6A (i.e. X corresponds to fragment ***A*** when bound at the position bearing label V). This evidence alone was not secure, and further data interpretation was therefore required.

Editing of the ^{13}C-{^{1}H} NMR spectrum *via* 2D [^{1}H, ^{13}C] HSQC data made it clear that the remaining 10 carbon-13 NMR resonances were associated with quaternary (non-protonated) carbons, providing a significant challenge for structure elucidation.

2D [^{1}H, ^{13}C] HMBC NMR data were therefore used by combining three sets of data from small (3 Hz), medium (7 Hz) and large (12 Hz) long-range $^{n}J_{HC}$-coupling optimization conditions. Smaller couplings result from longer-range correlations between more remote carbon and proton centres compared with medium and large sized couplings. However, distinguishing the number of intervening bonds associated with a given cross-peak in HMBC NMR data can be challenging and ambiguous. This is because $^{2}J_{HC}$, $^{3}J_{HC}$ and $^{4}J_{HC}$ couplings can give rise to cross-peaks that coexist within the same data sets. For n > 1, $^{n}J_{HC}$ correlations can be observed in the same context as $^{1}J_{HC}$ correlations when HSQC and HMBC data sets are combined (Fig. 5B).

From the 3 Hz optimized data, two additional HMBC correlations emerged compared with the other data sets that revealed through-bond relationships according to resonance pairs (**D, a**) and (**E, a**). The chemical shift of carbon resonance **a** is typical of a carbonyl carbon. It was concluded that protons **D** and **E** were, therefore in bonding proximity to a carbonyl carbon centre. No HMBC correlations were observed to the carbon-13 resonance designated **h**, making this a challenging carbon centre to identify within the structure of **1**. Given the likelihood of a mixture of $^{2}J_{HC}$ and $^{3}J_{HC}$ within these data and the strong possibility of mis-assignment taking place without further supporting information, it was considered prudent to acquire and interpret 2D [^{13}C, ^{13}C] INADEQUATE NMR data. Such data re used to directly map the carbon-carbon skeleton of a molecule through $^{1}J_{CC}$ couplings at natural ^{13}C-

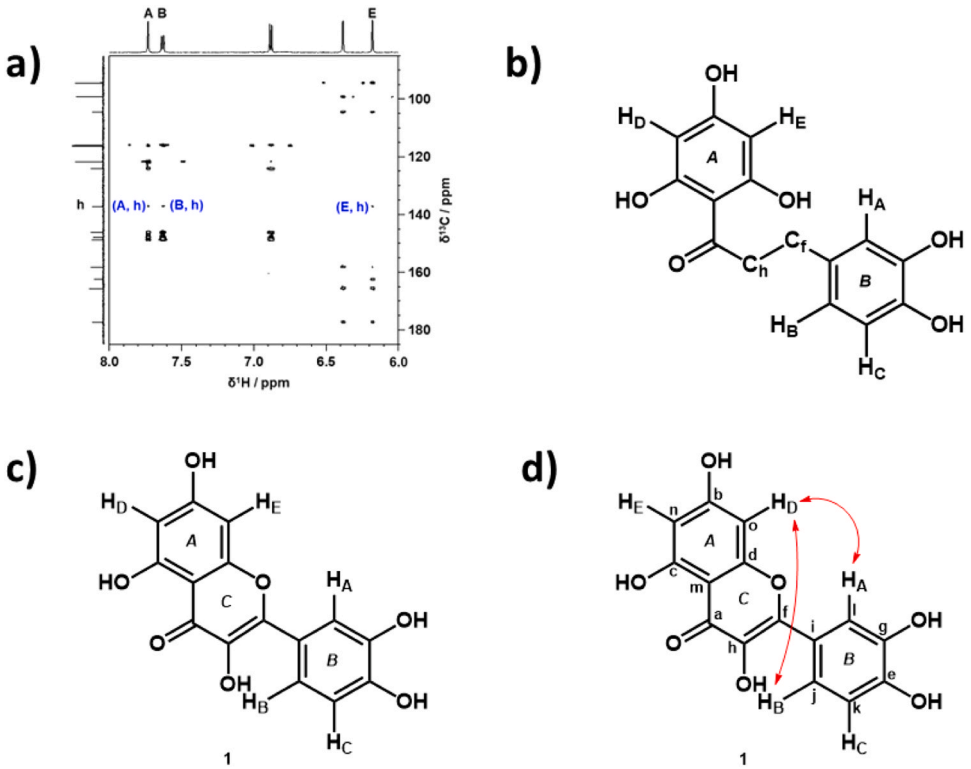

Fig. 7. Data to final structure. **a)** 600 MHz 2D [^{1}H, ^{13}C] HMBC NMR data optimized for 3 Hz $^{n}J_{HC}$ and acquired with traditional t_1 incrementation. Assignment of key correlations are indicated (see text for details). **b)** Fragment connection arising from 2D [^{1}H, ^{13}C] HMBC NMR correlation evidence. **c)** Characteristic substitution pattern and double bond connections.

isotopic abundance.

Applying the 13–13C one bond relationships defined by the 2D INADEQUATE NMR data to the molecular fragments defined to this point allowed a framework to be defined based on the starting evidence of all CH correlations determined from 2D [^{1}H, ^{13}C] HSQC and HMBC NMR (Fig. 7A).

To extend to an understanding of the likely functional group substitution of these fragments, chemical shift considerations were used. Both **D** and **E** appeared at lower chemical shift within the typical region identified for aromatic proton resonances, namely at δ ^{1}H = 6.386 ppm and 6.182 ppm, i.e. significantly shielded compared with the reference proton chemical shifts of benzene in CD_3OD (δ ^{1}H = 7.33 ppm). This suggested the presence of an adjacent electron-donating group. Consideration of carbon-13 NMR chemical shifts of the carbons to which these protons were attached (δ^{13}C(**o**) = 94.41 ppm, δ^{13}C(**n**) = 99.24 ppm) was also in keeping with this suggestion, with significant shielding compared with the carbon-13 chemical shift of benzene in CD_3OD (δ^{13}C = 129.34 ppm). By comparison, the carbon centre lying between those for whom the carbon-13 signal assignments were **o** and **n**, namely carbon signal **b**, appeared at a resonance position δ ^{13}C = 162.5 ppm, i.e. significantly deshielded and having the highest chemical shift of any carbon centre within the molecule except for **a**. The combined evidence suggested that U (Fig. 6A) had the functional group identity of -OH, which has both deshielding (for immediately attached) and shielding effects (for *ortho* centres) in the surrounding structural neighbourhood. By the same token, both **c** and **d** were similarly significantly deshielded and were confidently attached to oxygen centres. This provided the extended framework shown (Fig. 6B).

Referring to the 2D [^{1}H, ^{13}C] HMBC NMR data, correlations (**D**, **a**) and (**E**, **a**) corresponded to $^{4}J_{HC}$ coupling between the carbonyl carbon centre and the protons *ortho* to the phenolic group attached at carbon **b**. By association, both $^{2}J_{HC}$ and $^{3}J_{HC}$ correlations were identified in the 2D [^{1}H, ^{13}C] HMBC NMR data for the same fragment, building confidence for the correct arrangement and assignment of atoms within this ring.

For the adjacent ring, ***B***, similar chemical shift arguments were applied. Hence, carbon resonances **e** and **g** at δ^{13}C = 148.77 ppm and 146.22 ppm respectively, were associated with carbons directly attached to oxygen based on deshielding effects, whereas adjacent carbons **k** and **l**, with carbon resonances at δ ^{13}C = 116.23 ppm and 116.00 ppm, were considered to be shielded through electron donation into the ring by the neighbouring oxygens as shown.

How are the two fragments connected to create a single molecule framework? To address this, 3 Hz optimized 2D [^{1}H, ^{13}C] HMBC NMR data were acquired using a traditional acquisition approach rather than *via* non-uniform sampling. The former holds better scope for detecting weak correlations associated with longer-range couplings. In these data (Fig. 7A), three key correlations were observed: (**A**, **h**), (**B**, **h**) and (**E**, **h**).

Although no $^{1}J_{CC}$ correlation was observed between **f** and **h**, the suggestion from these HMBC data is that these carbons are connected, resulting in the appearance of long-range ($^{4}J_{HC}$ and $^{5}J_{HC}$) correlations as shown. The result of such a connection would place **A** and **B** at a distance from **D**, calling into question the NOE results, as indicated in the figures by the red double headed arrows. This conflicting evidence can be accounted for through alternative considerations as described below.

The remaining question concerned the character by which carbons **h** and **f** were substituted. Since both atoms are sp^{2} hybridized, and since no further non-exchangeable protons were evidenced within the NMR data, it followed that connection to oxygen would be logical and when combined with double-bond character between the two centres and considering the likely chemistry occurring to stabilize the structure, the conclusion which is drawn is that **1** corresponds closely to the structure shown at Fig. 7C.

To check the feasibility that the elucidated structure is consistent with these NMR data, two approaches were adopted. Firstly, chemical shift prediction algorithms were used according to procedures available at www.nmrdb.org(26−28) [23,24] and through ChemDraw (PerkinElmer Informatics, Inc., Professional Version 19.0.0.22) and *via* the MestreNova prediction module (MestreNova Version 14.3.3–33362, Mestrelab Research S.L.) in order to compute the likely carbon-13 chemical shifts for **1**. A comparison between calculated and experimental results is shown in Table 1 alongside experimental results for a sample of Quercetin solubilized in CD_3OD and analysed by carbon-13 NMR spectroscopy at different magnetic field strengths [25].

These data show such similarity that the likelihood of the compound not being **1** is unlikely in the extreme. Precedent for **1** exists, the compound being Quercetin, a flavonol of molecular formula $C_{15}H_{10}O_7$, a pigmenting molecule found in many edible plants.

An aspect of NMR data assignment and interpretation, alongside the human factors associated with such a process are worth commenting on at this point. The literature associated with the interpretation of NMR spectra and subsequent structure elucidation of natural products by this approach is littered with errors, misinterpretations, and incorrect structure propositions [27]. This is not only due to ambiguities that may arise when interpreting particular types of NMR spectra, including 2D [^{1}H, ^{13}C] HMBC, 2D [^{1}H, ^{1}H] COSY and 2D [^{1}H, ^{1}H] TOCSY NMR spectra. It is also to do with human factors and the mindset of the investigator, which is notorious for its inability to adapt to alternative modes of thinking and interpretation once a particular line of investigation has been adopted [28]. In the current case, the assignment of the ***A*** ring presented one of two options. As shown (Fig. 7C) this results in an ***A*** ring orientation such that $\mathbf{H_E}$ and $\mathbf{H_A}$ are in close proximity to one another. However, the NOE data do not support this orientation: $\mathbf{H_A}$ and $\mathbf{H_B}$ do not show NOE to $\mathbf{H_E}$, but instead, they show NOE to $\mathbf{H_D}$. To fit the data, therefore, requires orientating the ***A*** ring as its mirror image relative to that shown previously (see Fig. 7D).

Hence, the definitive ^{1}H and ^{13}C NMR data assignments for **1** are shown combined with a fit of the observed NOE data.

4.3. DILP gene expression studies

From our gene expression studies, we speculate that PC might be acting via a more interesting mechanism that could be of benefit clinically. DILP2 and DILP5 are involved in the homeostasis of carbohydrates and protein, including fats. On the other hand, the activity of PC on DILP2 and DILP5 was similar to those with standard antidiabetic drugs. This is in agreement with the report of Woo *et al.*, [30] which suggests that glibenclamide, a potent inhibitor of SUR1-TRPM4 channels, is transcriptionally upregulated in cerebral ischemia and also increases the expression of peptides. However, our observation justifies the hypoglycaemic effects of PC in type 2 diabetes (Fig. 8A and C). DILP2 and DILP5 are highly conserved between Drosophila and man [18]. The similarity between human and insulin signalling pathways presents a strong benefit for the use of Drosophila to investigate potential anti-diabetic drugs. The similarity between standard drugs and PC in the gene expressions justifies this experiment and its use in alternative medicine.

PC is used in the treatment of type 2 diabetes in sub-Saharan Africa. Quercetin obtained from the ethyl acetate fraction of the leaf of PC partially clarifies the mechanism of effects of decoction from PC in diabetes management in alternative medicine. The ameliorating effects of quercetin on diabetes and its complications have been extensively described as a possible multi therapy [31]. This experiment could potentially add value to the science of phytomedicine, as well as the acclaimed use of *P. curatellifolia* in traditional medicine and the development of antidiabetic drugs.

5. Conclusion

We conclude that the leaf extract of *Parinari curatellifolia* exhibits hypoglycaemic effects that justify its use in alternative medicine to manage type 2 diabetes. The ethyl acetate fractions of the leaves of *P. curatellifolia* contain a high amount of quercetin that exhibits

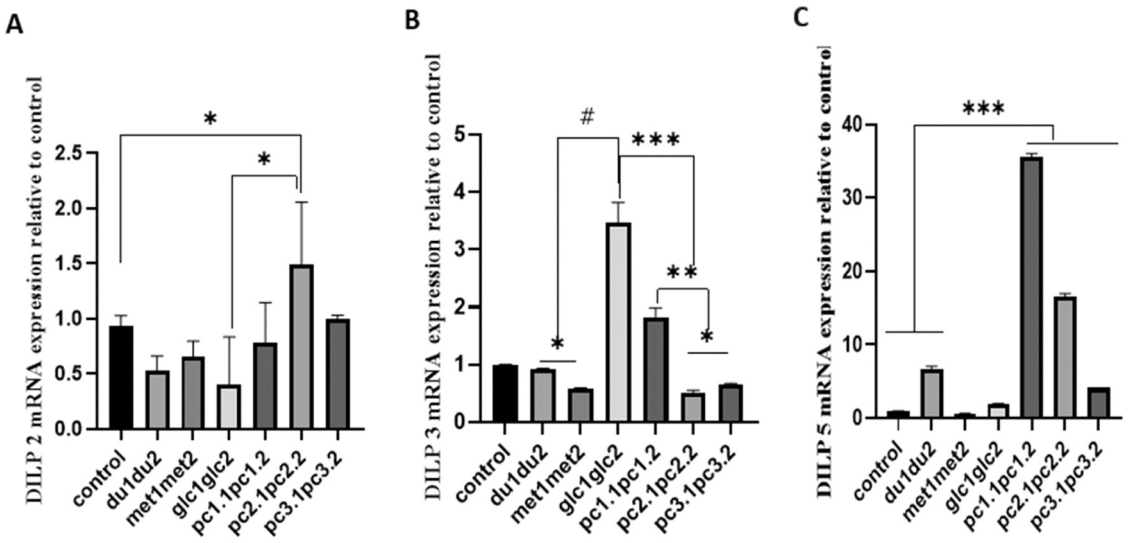

Fig. 8. (A) Showing significant ($P < 0.05$) increase in the *D. melanogaster* DILP2 gene expression by pc2 50 mg/10 g diet and glc1 0.05 mg/10 g diet. (B) showing no significant ($P > 0.05$) effects on the DILP3 gene expression with the control group but varying increases among the groups (C) significant increase ($P < 0.05$) in the DILP5 gene expression in the *Drosophila melanogaster* exposed to PC 10 mg and 50 mg/ 10 g diet. Our experiments show that compounds from *P. curatellifolia* significantly expressed DILP2 and DILP5 as possible mechanisms of its antihyperglycemic effects in type 2 diabetic *D. melanogaster*. DILP 2 and DILP5 are highly conserved in the Drosophila and humans, hence explaining the reason for the use of PC in alternative medicine to treat type 2 diabetes.

antioxidant and antidiabetic effects in the hyperglycaemic Drosophila. From this study, we hypothesized that the phytocompounds of *P. curatellifolia* exert their hypoglycaemic properties through binding to the Drosophila insulin-like peptide (DILP) II and V, resulting in the phosphorylation of insulin down regulatory pathways that could lead to the translocation of the glucose transporters to the cell surface and glucose disposal. The most abundant compound active against diabetes in the ethyl acetate fraction of the leaf of PC was attributed mainly to quercetin.

CRediT authorship contribution statement

Simeon O (SO): Research design, investigation, Drosophila bench work implementation, fractionation and isolation, Data collection and analysis, manuscript writing, and funding acquisition. John CA (JCA): Project coordination, Standard Operating Procedure adherence, monitoring, and funding aquisition. Aboi JKM (AJKM): Development of SOP, overall project management, and editing of the manuscript. Taiwo EA (TEA): Project oversight of isolation, characterization, day-to-day management of activities, and correction of the manuscript. Titilayo OJ (TOJ): Support of the Drosophila model benchwork and manuscript editing. Pam DL (PDL): Design, coordinate, and investigate the gene expression study and manuscript writing. Chuwang JN (CJN): Support in the primer design, implementation of the gene expression study, and editing of the manuscript. Nnaemeka EN (NEN): Support in the design, implementation of the gene expression studies, and editing of the manuscript. Francis MA (FMA): Supporting the fractionation and isolation of the compound. Uchechukwu O (UO): Data curation and analysis. Sunshine O (SO): Drosophila culture, handling, and sample preparation. Patricia TC (PTC): Drosophila treatment, sample preparation, and biochemical analysis. Gwyn GWG (GWG): Collaboration platform between the University of Jos and the Strathclyde Institute of Pharmacy and Biological Sciences (SIPBS), University of Strathclyde, and for editing and review of the entire manuscript. John AP (JAP): NMR spectroscopy data acquisition, processing, analysis, data interpretation and manuscript writing.

Ethical consideration

All experiments were performed with standard specifications. However, experiments involving the fruit fly does not necessarily require strict ethical approval.

Funding sources

This work was supported by a research fund from the Nigerian Tertiary Education Trust Fund (TETFund) intervention scheme with grant number TETF/ES/DR&D-CE/NRF2020/SETI/37/VOL.1. We also acknowledge EPSRC/UKRI funding to support NMR spectroscopy at 800 MHz under Grant EP/R030065/1.

Declaration of Generative AI and AI-assisted technologies in the writing process

The authors declared that no generative AI was used to prepare any part of this manuscript.

Declaration of Competing Interest

The authors declare the following financial interests/personal relationships which may be considered as potential competing interests: Simeon Omale and John Parkinson reports financial support was provided by Tertiary Education Trust Fund and EPSRC/UKRI funding . If there are other authors, they declare that they have no known competing financial interests or personal relationships that could have appeared to influence the work reported in this paper.

Acknowledgement

The authors acknowledge the contribution of the staff of the Africa Centre of Excellence in Phytomedicine Research and Development (ACEPRD), University of Jos, Nigeria, for providing bench space and the use of their *Drosophila melanogaster* laboratory, as well as human resource support. We also appreciate the support from the members of staff of the Biotechnology division of the National Veterinary Research Institute (NVRI), Vom Nigeria. Finally, we thank the NMR team of the Department of Pure and Applied Chemistry, Thomas Graham Building, University of Strathclyde, Glasgow, United Kingdom.

Data availability

Data will be made available on request.

References

[1] R. Williams, S. Karuranga, B. Malanda, P. Saeedi, A. Basit, S. Besançon, C. Bommer, A. Esteghamati, K. Ogurtsova, P. Zhang, Global and regional estimates and projections of diabetes-related health expenditure: results from the International Diabetes Federation Diabetes Atlas, Diabetes Res. Clin. Pract. 162 (2020) 108072, https://doi.org/10.1016/j.diabres.2020.108072.

[2] S.K. Jayaswal, S. Singh, P.S. Malik, S.K. Venigalla, P. Gupta, S.N. Samaga, R. N. Hota, S.S. Bhatia, I. Gupta, Detrimental effect of diabetes and hypertension on the severity and mortality of COVID-19 infection: a multi-center case-control study from India, Diabetes Metab. Syndr. 15 (5) (2021) 102248, https://doi.org/10.1016/j.dsx.2021.102248.

[3] M. Eddouks, D. Chattopadhyay, V. De Feo, W.C. Cho, Medicinal plants in the prevention and treatment of chronic diseases, Evid. Based Compliment. Altern. Med. (2012) 458274, https://doi.org/10.1155/2012/458274.

[4] A.B. Shori, Screening of antidiabetic and antioxidant activities of medicinal plants, J. Integr. Med. 13 (5) (2015) 297–305, https://doi.org/10.1016/s2095-4964(15)60193-5.

[5] R. Usai, S. Majoni, F. Rwere, Natural products for the treatment and management of diabetes mellitus in Zimbabwe-a review, Front. Pharm. 2045 (2022) 1–21, https://doi.org/10.3389/fphar.2022.980819.

[6] S. Ogbonnia, Extracts of mobola plum (*Parinari curatellifolia* Planch ex Benth, Chrysobalanaceae) seeds and multiple therapeutic activities, Nuts seeds Health Dis. Prev. (2010) 767–774, https://doi.org/10.1016/B978-0-12-375688-6.10091-X.

[7] S. Omale, A. Auta, S. Banwat, K. Amagon, Y. Thomas, Effects of the ethanolic extract of *Parinari curatellifolia* on cat blood pressure and rabbit jejunum preparations, Int. J. Parm. Res. 1 (2) (2011) 39–44.

[8] O.O. Crown, T.R. Komolafe, A.C. Akinmoladun, M.T. Olaleye, A.A. Akindahunsi, A. A. Boligon, *Parinari curatellifolia* seed flavonoids protect against Triton-induced dyslipidemia and atherogenicity in rats, Tradit. Kamp. Med. 5 (1) (2018) 11–18, https://doi.org/10.1002/tkm2.1082.

[9] S. Ogbonnia, G. Mbaka, E. Anyika, O. Lediju, D. Ota, Evaluation of the effects of *Parinari curatellifolia* seed and *Anthocleista vogelli* root extracts individually and in combination on postprandial and alloxan-induced diabetes in animals, Planta Med. 77 (12) (2011) PF45, https://doi.org/10.1055/s-0031-1282433.

[10] Y. Ogunbolude, M. Ajayi, T. Ajagbawa, A. Igbakin, J. Rocha, I. Kade, Ethanolic extracts of seeds of *Parinari curatellifolia* exhibit potent antioxidant properties: a possible mechanism of its antidiabetic action, JPP 1 (6) (2009) 067–075.

[11] M.T. Olaleye, A.E. Amobonye, K. Komolafe, A.C. Akinmoladun, Protective effects of *Parinari curatellifolia* flavonoids against acetaminophen-induced hepatic necrosis in rats, Saudi J. Biol. Sci. 21 (5) (2014) 486–492, https://doi.org/10.1016/j.sjbs.2014.06.005.

[12] M. Gororo, T. Chimponda, E. Chirisa, S. Mukanganyama, Multiple cellular effects of leaf extracts from *Parinari curatellifolia*, BMC Complement. Altern. Med. 16 (1) (2016) 305, https://doi.org/10.1186/s12906-016-1287-6.

[13] S.O. Ogbonnia, A. Adekunle, S.O. Olagbende-Dada, E.N. Anyika, V.N. Enwuru, M. Orolepe, Assessing plasma glucose and lipid levels, body weight and acute toxicity following oral administration of an aqueous ethanolic extract of *Parinari curatellifolia* Planch,(Chrysobalanaceae) seeds in alloxan-induced diabetes in rats, Afr. J. Biotechnol. 7 (17) (2008) 2998–3003, https://doi.org/10.5897/AJB08.469.

[14] S. Omale, J.C. Aguiyi, O.G. Adekunle, T.O. Johnson, S.O. Ochala, M.A. Etuh, M. C. Eze, Evaluation of antidiabetic effects of the stem bark extract of *Parinari curatellifolia* (Planch. ex Benth.) in *Drosophila melanogaster*, J. Pharmacol. Toxicol. 16 (2021) 9–21, https://doi.org/10.3923/jpt.2021.9.21.

[15] E. van Dam, L.A. van Leeuwen, E. Dos Santos, J. James, L. Best, C. Lennicke, A. J. Vincent, G. Marinos, A. Foley, M. Buricova, Sugar-induced obesity and insulin resistance are uncoupled from shortened survival in Drosophila, Cell. Metab. 31 (4) (2020) 710–725, https://doi.org/10.1016/j.cmet.2020.02.016.

[16] Y.H. Inoue, H. Katsube, Y. Hinami, Drosophila models to investigate insulin action and mechanisms underlying human diabetes mellitus, Adv. Exp. Med. Biol. 1076 (2018) 235–256, https://doi.org/10.1007/978-981-13-0529-0_13.PMID:29951823.

[17] Y. Miao, R. Chen, X. Wang, J. Zhang, W. Tang, Z. Zhang, Y. Liu, Q. Xu, *Drosophila melanogaster* diabetes models and its usage in the research of anti-diabetes management with traditional Chinese medicines, Front. Med. 9 (2022) 953490, https://doi.org/10.3389/fmed.2022.953490.

[18] S. Post, G. Karashchuk, J.D. Wade, P. De Meyts, M. Tatar, Drosophila insulin-like peptides DILP2 and DILP5 differentially stimulate cell signaling and glycogen phosphorylase to regulate longevity, Front. Endocrinol. (Lausanne) 28 (9) (2018) 245, https://doi.org/10.3389/fendo.2018.00245.

[19] Y. Wang, C. Dawid, G. Kottra, H. Daniel, T. Hofmann, Gymnemic acids inhibit sodium-dependent glucose transporter1, J. Agric. Food Chem. 62 (25) (2014) 5925–5931, https://doi.org/10.1021/jf501766u.

[20] J.M. Tennessen, W.E. Barry, J. Cox, C.S. Thummel, Methods for studying metabolism in Drosophila, Methods 68 (1) (2014) 105–115, https://doi.org/10.1016/j.ymeth.2014.02.034.

[21] C.E. Ogwuche, J.O. Amupitan, G.I. Ndukwe, Evaluation of antimicrobial activities of isolated compounds from the leaf of the white specie of *Sesamum indicum* from Benue State, Nigeria, JASEM 18 (4) (2014) 568–574, https://doi.org/10.4314/jasem.v18i4.2.

[22] S.N.S. Morris, C. Coogan, K. Chamseddin, S.O. Fernandez-Kim, S. Kolli, J.N. Keller, J.H. Bauer, Development of diet-induced insulin resistance in adult *Drosophila melanogaster*, Biochim. Biophys. Acta 1822 (8) (2012) 1230–1237, https://doi.org/10.1016/j.bbadis.2012.04.012.

[23] D. Banfi, L. Patiny, www. nmrdb. org: resurrecting and processing NMR spectra on-line, Chimia 62 (4) (2008), https://doi.org/10.2533/chimia.2008.280, 280-280.

[24] C. Steinbeck, S. Krause, S. Kuhn, NMRShiftDB constructing a free chemical information system with open-source components, J. Chem. Inf. Comput. Sci. 43 (6) (2003) 1733–1739, https://doi.org/10.1021/ci0341363.

[25] S. Dall'Acqua, G. Miolo, G. Innocenti, S. Caffieri, The photodegradation of quercetin: relation to oxidation, Molecules 17 (8) (2012) 8898–8907, https://doi.org/10.3390/molecules17088898.

[26] E. Wenker, H.E. Gottlieb, Carbon-13 nuclear magnetic resonance spectroscopy of flavonoid and isoflavonoid compounds, Phytochem 16 (11) (1977) 1811–1816, https://doi.org/10.1016/0031-9422(71)85095-1.

[27] D.C. Burns, W.F. Reynolds, Minimizing the risk of deducing wrong natural product structures from NMR data, J. Magn. Reson 59 (5) (2021) 500–533, https://doi.org/10.1002/mrc.4933.

[28] C. Szantay Jr. Anthropic awareness: the human aspects of scientific thinking in NMR spectroscopy and mass spectrometry, 1st Edition, Elsevier, 2015. ISBN: 9780124199637.

[29] M. Janice, J. Joel, H. Holly, E.H. Beatriz, B.W. Keeey, Nelson Paul, N. Mani, Bioassay-guided fractionation protocol for identifying novel active compounds in selected Australian flora Plants, Plants (Basel) 11 (21) (2022) 2886, https://doi.org/10.3390/plants11212886.

[30] S.K. Woo, N. Tsymbalyuk, O. Tsymbalyuk, S. Ivanova, V. Gerzanich, J.M. Simard, SUR1-TRPM4 channels, not KATP, mediate brain swelling after cerebral ischemia, Neurosci. Lett. 718 (2020) 134729, https://doi.org/10.1016/j.neulet.2019.134729.

[31] R. Dhanya, Quercetin for managing type 2 diabetes and its complications, an insight into multitarget therapy, Biomed. Pharmacother. 146 (2022) 112560, https://doi.org/10.1016/j.biopha.2021.112560.